# Water Fastness of Ink Jet Prints on Modified Conventional Coatings

**Katri Vikman▲* and Tapani Vuorinen**

*Helsinki University of Technology, Laboratory of Forest Products Chemistry, Espoo, Finland*

In order to produce color ink jet prints with good fastness properties, the use of special, coated papers is generally essential. The use of modified conventional coating pigments has been suggested as a means to obtain a matte ink jet coating that would combine the good properties of silica-based ink jet coatings and conventional printing papers. This study examined the water fastness of ink jet prints using experimental coated papers containing modified PCC and kaolin pigments, and model inks with known compositions. The properties of the coatings were altered by using different ratios of coating pigments, and types of binder and dispersant. The water fastness of the prints was analyzed using conventional methods for measuring paper properties and print quality, combined with FTIR and Raman spectroscopy and multivariate data analysis methods. The results indicated that within the studied sample sets, primarily the chemical paper–ink interactions contributed to water fastness on cationic PVA-poly-DADMAC coatings, whereas on weakly cationic styrene-acrylate latex-starch coatings, structural paper properties were relevant as well. In general, increased impermeability of the coating appeared to be advantageous. With regard to the chemical paper–ink interactions, ionic bonding between the dye and the coating proved to be beneficial for water fastness, provided that the interacting coating component was insoluble to water.

Journal of Imaging Science and Technology 48: 138–147 (2004)

## Introduction

The current trend towards color printing and the development of fast ink jet printers have created an increasing need for coated ink jet papers.[1] High end ink jet coatings are generally based on silica pigments, a polyvinyl alcohol binder (PVA) and a cationic polymer additive. Such media provide excellent print quality by enabling rapid and efficient fixation of the anionic ink jet colorants to the coating.[2–7] However, certain disadvantages limit more widespread use of them. First of all, silica grades are typically rather expensive owing to their costly ingredients and the need to use relatively slow coating methods because of the low viscosity and considerable need for binder of the coating colors. Consequently, large-scale printing on silica coatings is uneconomical. Furthermore, silica grades are generally rather poorly applicable to printing processes other than ink jet, which excludes their use for example in modern hybrid printing presses.[3,4,6,8,9] In consequence, other lower-cost types of coating are being sought to replace silica grades.

Coating components typically used for conventional printing papers are not applicable to ink jet printing as such because of their small affinity to anionic ink jet dyes and inadequate absorption capacity. Thus, improvements in ink jet print quality require modification of the pigment or polymer composition used in conventional coatings.[3–6,10,11] Several approaches have been presented to obtain a coating that would integrate the absorption properties of the silica coatings and the lower cost of conventional coatings. For example, the use of ground or precipitated calcium carbonate and surface-enhanced aluminosilicate (SEAS) as a substitute for silica pigments has been suggested,[2,12,13] as well as modification of traditional offset coating formulations with bentonite and PVP copolymer.[11] The use of cationic starch in ink jet coatings combined with conventional pigments[1,4] has also been proposed.

In order to achieve good long-term ink jet print quality with such novel modified coatings, knowledge of the underlying mechanisms of fastness properties is essential. In an earlier study, the effects of the coating polymer composition on the water fastness of ink jet prints on coatings based on conventional kaolin was investigated.[14] The results of this study suggested that both the physical properties of the coating and chemical paper–ink interactions contribute to water fastness. In general, increased structural impermeability of the coating was suggested to be beneficial. Ionic interactions between the colorant and coating appeared to be favorable for water fastness on hydrophilic coatings. Another study[15] indicated that the water fastness of ink jet prints could be improved if modified PCC and kaolin were used as coating pigments instead of conventional kaolin. The magnitude of enhancement was, however, dependent both on the type of colorant and the coating polymer system used.

The present study attempts to further examine factors contributing to the water fastness of ink jet prints

Original manuscript received December 3, 2004

▲ IS&T Member

* katri.vikman@hut.fi

**TABLE I. Compositions of Model Coatings.**

| Coating | PCC:Kaolin Ratio (pph) | Binder | Dispersant | Coating Color pH |
|---|---|---|---|---|
| P0:100 | 0:100 | PVA 10 pph | Poly-DADMAC 3 pph | 10.4 |
| P20:80 | 20:80 | | | 10.1 |
| P40:60 | 40:60 | | | 9.9 |
| P60:40 | 60:40 | | | 9.9 |
| P80:20 | 80:20 | | | 9.5 |
| P100:0 | 100:0 | | | 8.2 |
| S0:100 | 0:100 | Weakly cationic SA latex 10 pph | Weakly cationic starch 4 pph | 10.2 |
| S20:80 | 20:80 | | | 10.0 |
| S40:60 | 40:60 | | | 9.9 |
| S60:40 | 60:40 | | | 9.6 |
| S80:20 | 80:20 | | | 9.0 |
| S100:0 | 100:0 | | | 8.1 |

on coatings consisting of modified coating pigments. The contribution of the physical properties of the coating and chemical paper–ink interactions are of particular interest.

## Experimental

### Model Coatings

The focus of the experimental work was on the influence of the pigment composition of the coating on water fastness. Consequently, a model coating set was generated, where the structure of the coating layer, absorption properties and net-charge were altered by varying the pigment and polymer compositions (Table I). The coating pigments were precipitated calcium carbonate (PCC, Jetcoat 30 from Specialty Minerals) and kaolin (Digitex from Engelhard), both intended for use particularly in ink jet coatings. Both pigments were used as received: PCC as a slurry with 25% solids content, consisting of pigment and carboxymethyl cellulose (CMC) as a thickener, and the kaolin as a pigment powder. According to the manufacturer, the structure of this kaolin grade is modified both on the surface and internally, such that the surface area and pore volume are increased in comparison with conventional platy kaolins. Moreover, the modification was reported to include removal of most of the Si present in kaolin.

The absorption properties of the coatings were modified using different types of binder. These were polyvinyl alcohol (PVA, Celvol 107 from Air Products, degree of hydrolysis 98.0–98.8%) and weakly cationic styrene acrylate latex (SA, Raiprint 300 from Raisio Chemicals, charge 236 $\mu$mol $kg^{-1}$ at pH 8). According to the manufacturer, the latex is stabilized with a cationic starch. The net charge of the coatings and thus the propensity to bind anionic dyes was varied using different dispersants for the kaolin pigment. These were cationic polydiallyl dimethyl ammonium chloride (poly-DADMAC, Cartafix VXT from Clariant International Ltd., cationic charge density 2200 mEqkg$^{-1}$) and weakly cationic starch (Raisamyl 402 from Raisio Chemicals, DS = 0.018, cationic charge density 100 mEqkg$^{-1}$ ). Moreover, 1.5 pph of CMC (Finnfix 10 from Noviant, DS = 0.6 – 0.95) was added to each coating color to increase its viscosity. The coating colors were nevertheless very fluid, which complicated the coating process and may also have caused some unexpected variation in the properties of the final coating layer. The pH of the coating colors was not adjusted. The base paper was surface-sized copy paper (80 gm$^{-2}$) and the target amount of coating was 10 gm$^{-2}$. The coating was made with a CLC laboratory blade coater at a 50° blade angle and a coating speed of 350 m/min. The coated papers were not calendered.

The surface charge of the PCC and kaolin pigments was described by measuring the zeta potential with a laser-based multiple-angle particle electrophoresis analyzer, Coulter Delsa 440 from Langley Ford Instruments. Prior to the measurements, kaolin powder was suspended in deionized water to obtain a slurry with 25% solids content. The measurement was made by mixing a few droplets of the 25% pigment slurry into 50 ml of deionized water. The run parameters in the zeta potential measurements were: 5 V electric field, 500 Hz frequency range and 120 s measurement time.

The porosity characteristics of the final coated papers were measured with a Bendtsen air permeability measurement device (the SCAN-P 60:87 standard) and with mercury porosimetry using an Autopore III 9410 from Micromeritics. The average pore diameter and total pore area were used as parameters in analyzing the results. Roughness was measured with a Mitutoyo Surftest 401 profilometer and with the Bendtsen method (the SCAN-P 21:67 standard). The profilometric roughness parameters were $R_a$ (the arithmetic mean of the deviations of the roughness profile from the mean line) and theta angle $\theta_a$ (the mean slope of the topological profile of paper). The contact angle measurements were made using the sessile drop method.[14]

### Model Inks

The model ink formulations and the data on model ink properties are shown in Table II. Two soluble azo colorants with different chemical properties and one pigment dispersion were chosen for the inks. These were CI Direct Yellow 86 (DY 86), CI Direct Violet 107 (DV 107) and CI Pigment Yellow 83 (PY 83). Detailed information on the molecular structure of DY 86 and PY 83 can be found elsewhere, i.e., from the *Colour Index*. Information on the molecular structure of DV 107 is not publicly available. The dye-based colorants were purchased from Avecia Ltd as aqueous solutions, and the pigment dispersion from Clariant International Ltd. The latter contained 35% of colorant (average particle size 40 nm) and 15% of 1,2-propylene glycol (PG), whereas the exact compositions of the dye solutions are not known. The added co-solvents were 2-pyrrolidone (2-p, purity grade: purum; ≥ 99.0% GC), diethylene glycol (DEG, purum; ≥ 98.0% GC) and tetraethylene glycol (TEG, purum; ≥ 97% GC), all from Sigma-Aldrich.

The inks were analyzed to determine their pH using a Schott pH meter, surface tension using a Sigma 70 computer-controlled automatic surface tension meter

**TABLE II. Compositions and Properties of Model Inks.**

| Ink Code | Colorant Type | Added Co-solvent | | Distilled Water, wt. % | pH | Surface Tension, mN*m$^{-1}$ | Viscosity, mPas |
|---|---|---|---|---|---|---|---|
| | | Type | Amount, wt. % | | | | |
| DY86 2p1 | DY 86 | 2-p | 10 | 86 | 7.75 | 58.13 | 2.41 |
| DY86 2p2 | DY 86 | 2-p | 20 | 76 | 7.50 | 56.84 | 2.75 |
| DY86 DEG | DY 86 | DEG | 10 | 86 | 7.96 | 52.08 | 2.54 |
| DY86 TEG | DY 86 | TEG | 10 | 86 | 7.47 | 58.53 | 2.77 |
| DV107 | DV 107 | 2-p | 20 | 76 | 8.12 | 37.76 | 2.79 |
| PY83 | PY 83 | PG | 15 | — | 7.75 | 43.97 | 1.83 |

(ring method), and viscosity using a Bohlin VOR rheometer. The model ink compositions used in this study were selected to simplify the analysis of paper–ink interactions. Consequently, they do not necessarily behave as typical commercial ink jet inks, as far as physical and chemical paper–ink interactions are concerned.

### Water Fastness Test

To examine the influence of the pigment and polymer composition of the coating on the water fastness of ink jet prints, solid single-color areas were printed on the model coatings with an Epson Stylus Photo 890 piezo ink jet printer using the model inks. In general, because the compositions of the model inks (Table II) were not optimized for the printer performance, the printed areas were extensively striped, instead of the ink being evenly spread over the paper surface. This unevenness may have caused unexpected variations in the measured print quality parameters. The exact amount of ink on the paper is unknown, and therefore only dye–paper interactions are considered in this study.

The water fastness of the prints was measured by immersing the printed samples into de-ionized water for 5 min without agitation, and allowing the immersed prints to dry for at least 5 hours at room temperature. Analogous methods have also been used in other studies.[6,16,17] The test conditions of the immersion method are rather severe, so the results might not necessarily correspond to the real conditions of print use. The advantage of this method, however, is that it enables an even exposure of the printed area to water. Color difference $\Delta E^*$ was used as a measure of water fastness, so CIEL*a*b* values were measured with a Minolta CM-1000 spectrophotometer from the unprinted papers and prints before and after exposing the prints to water. Average values of ten measurements were used in calculating color differences.

### Spectroscopic Measurements

To get more information on the chemical composition of the samples and on conceivable paper–ink interactions affecting light fastness, FTIR and Raman spectra of the coatings and prints were recorded.

The FTIR spectra of unprinted and printed coatings were recorded with a Bio-Rad FTS 6000 spectrometer using an ATR method with a diamond micro-crystal and a resolution of 8 cm$^{-1}$. In this method, the penetration depth of the IR beam[18] into the coating varies approximately in the range 0.2–1.4 μm, depending on the wavelength, the angle of the incident light beam ($\alpha$ = 45°), and the refractive indices of the ATR crystal ($n_1$ = 2.4) and the sample material (an approximate value for pigment coating $n_2$ = 1.55). In addition, variations in the contact between the crystal and the sample surface affect the penetration depth. To improve reproducibility, three measurements were made from each sample and the spectra were averaged. The FTIR spectra of the colorants and coating pigments were measured from dried samples with DTGS or rapid-scan PAS with a resolution of 8 cm$^{-1}$.

Raman depth profiling[19] of the prints was carried out with a dispersive Kaiser Raman Hololab 5000 spectrometer using a 785 nm diode laser, a 100X immersion objective, a spectral resolution of 4 cm$^{-1}$ and a depth profiling step of 1 μm. Intensive fluorescence of the kaolin-containing samples complicated Raman measurements and interpretation of the spectra.

### Multivariate Data Analysis Methods

The water fastness and spectral data were analyzed using projection methods, namely principal component analysis (PCA) and projection to latent structures (PLS). These methods make it easier to analyze multivariable, noisy and collinear data by presenting the observations as a swarm of points in a K-dimensional space (K is the number of variables), and projecting this swarm down onto a lower-dimensional hyperplane. The coordinates of the points on this hyperplane provide a compressed representation of all the observations, and the direction of the vectors of the hyperplane provide a corresponding representation of the variables. Consequently, the projection methods approximate the data as well as possible in the least squares sense. A detailed description of PCA and PLS, and their mathematical background can be found in the literature.[20] Multivariate data analysis methods have also been used in other studies, for example in characterization of pigments in coating formulations for high end ink jet papers[21] and in characterization of historic papers with FTIR-ATR spectroscopy.[22]

The effect of the physical properties of the coating on the water fastness was evaluated with projection to latent structures (PLS). The use of the PLS method for prediction and modeling purposes requires a large number of variables and observations in order to get reliable results. In the present study, the sample sets are rather small, so the calculated models should not be used in predicting water fastness values. However, the PLS analysis is justified here, as it gives a compact representation on the effects of all the studied X variables on all Y variables and their mutual relationships, thus making it easier to interpret the results.

Principal component analysis (PCA) was utilized in the interpretation of the FTIR-ATR spectra. Prior to making the PCA, the spectra from parallel measurements were averaged, but not ATR-corrected. Moreover, to get a more realistic impression of the contributions of various wavenumbers, unit variance scaling of the spectral data was not made. Accordingly, the obtained loading values are dependent on the intensities of corresponding FTIR bands and therefore do not directly depict the importance of the affiliated chemical group.

**TABLE III. Data on Paper Properties and Water Fastness. In the Paper Sample Notation, P Refers to the PVA-poly-DADMAC Coating Polymer System and S to the Latex-Starch Coating Polymer System.**

| Paper | Porosity | | | Roughness | | | Surface properties | | Water Fastness ΔE* (100h) | | | | | |
|---|---|---|---|---|---|---|---|---|---|---|---|---|---|---|
| | Bendtsen air perm. [ml/min] | Av. pore diameter [μm] | Total pore area [m²/g] | Bendtsen roughness [ml/min] | Ra [μm] | $\theta_a$ [deg.] | Polarity | Contact angle [° deg.] | DY86 2p1 | DY86 2p2 | DY86 DEG | DY86 TEG | DV107 | PY83 |
| P0:100 | 43 | 0.10 | 31.9 | 121 | 2.3 | 3.4 | 0.43 | 38.0 | 5.7 | 10.5 | 6.8 | 6.5 | 12.0 | 8.0 |
| P20:80 | 68 | 0.11 | 29.5 | 168 | 2.8 | 4.0 | 0.56 | 14.2 | 3.3 | 0.8 | 8.3 | 6.3 | 16.2 | 12.1 |
| P40:60 | 167 | 0.11 | 29.2 | 218 | 2.7 | 3.6 | 0.56 | 9.6 | 5.6 | 5.8 | 8.4 | 3.6 | 11.6 | 8.5 |
| P60:40 | 202 | 0.10 | 29.6 | 251 | 2.8 | 3.5 | 0.57 | 12.8 | 9.8 | 2.3 | 2.9 | 2.6 | 13.7 | 8.9 |
| P80:20 | 346 | 0.11 | 29.1 | 282 | 3.4 | 3.9 | 0.56 | 19.7 | 5.6 | 3.9 | 7.7 | 7.0 | 8.6 | 10.8 |
| P100:0 | 419 | 0.08 | 40.1 | 304 | 3.7 | 4.1 | 0.56 | 7.2 | 12.2 | 9.2 | 9.2 | 7.3 | 12.1 | 7.2 |
| S0:100 | 12 | 0.12 | 26.0 | 80 | 2.1 | 3.3 | 0.01 | 93.3 | 14.2 | 16.9 | 9.1 | 17.8 | 16.6 | 1.2 |
| S20:80 | 235 | 0.12 | 27.5 | 156 | 2.3 | 3.7 | 0.12 | 107.8 | 13.4 | 19.2 | 8.7 | 22.1 | 13.2 | 6.4 |
| S40:60 | 40 | 0.11 | 30.8 | 226 | 3.1 | 3.7 | 0.30 | 103.0 | 23.4 | 18.6 | 22.1 | 28.5 | 21.3 | 6.1 |
| S60:40 | 140 | 0.10 | 32.1 | 197 | 2.7 | 3.9 | 0.35 | 98.0 | 21.6 | 21.5 | 18.9 | 26.5 | 26.2 | 7.9 |
| S80:20 | 273 | 0.09 | 36.1 | 250 | 3.0 | 3.6 | 0.07 | 106.7 | 21.9 | 20.5 | 17.5 | 25.7 | 25.8 | 9.9 |
| S100:0 | 378 | 0.09 | 35.4 | 220 | 3.0 | 3.3 | 0.01 | 106.3 | 23.3 | 21.6 | 18.4 | 25.4 | 28.0 | 5.5 |

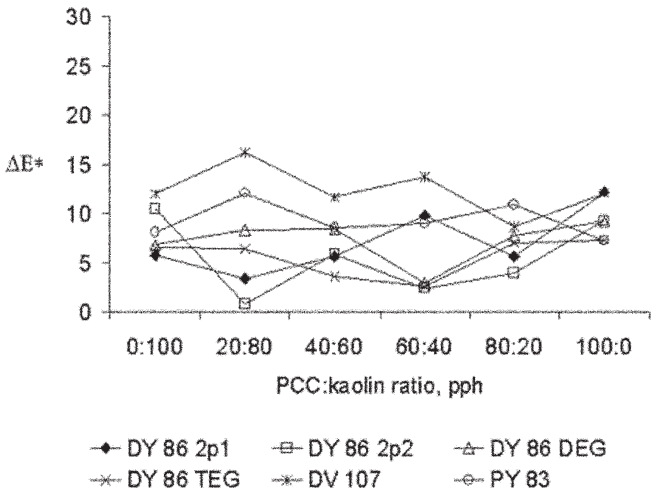


**Figure 1.** Water fastness of model inks on PVA-poly-DADMAC coatings. Large ΔE* denotes poor water fastness.

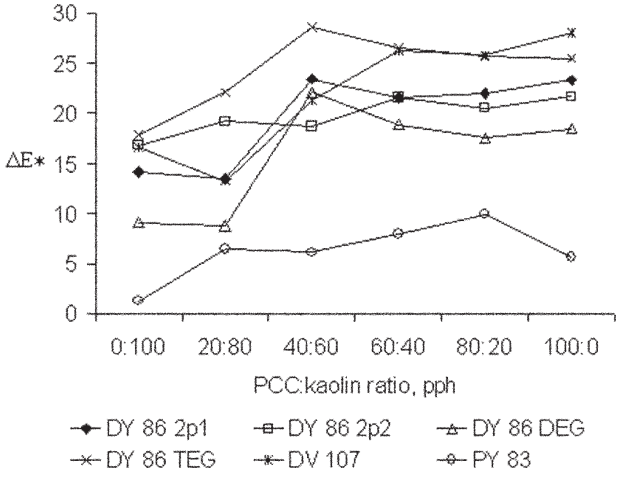


**Figure 2.** Water fastness of model inks on weakly cationic SA-latex-starch coatings. Large ΔE* denotes poor water fastness.

## Results and Discussion

### Effect of Physical Properties of Model Coatings

The data on paper properties and calculated water fastness values for the model coating set are presented in Table III. The water fastness of ink jet prints on PVA-poly-DADMAC coatings (P0:100…P100:0) and on weakly cationic latex-starch coatings (S0:100…S100:0) are presented as a function of the PCC:kaolin pigment ratio and ink composition in Figs. 1 and 2. It is evident that the water fastness of the studied dye-based model inks is generally significantly better on PVA-poly-DADMAC coatings than on weakly cationic SA latex-starch coatings, despite the clearly more hydrophobic nature of the latter. In contrast, the reverse is true for the pigmented ink PY 83, although the overall effect of the coating types appears to be smaller. On PVA-poly-DADMAC coatings, neither the pigment ratio of the coating, nor the ink composition, seem to have a marked influence on water fastness (Fig. 1). However, on weakly cationic latex-starch coatings (Fig. 2), both of these factors apparently contribute. On average, the water fastness of the studied inks deteriorates as the PCC:kaolin ratio increases. This behavior is particularly distinct with the dye-based inks, especially when the amount of PCC is increased from 0 to 40 pph. At larger PCC proportions, differences in water fastness values are leveled out.

A multivariate PLS analysis was run for the data in Table III to evaluate the effects of physical properties of the model coatings on water fastness. The six paper-related variables selected for the analysis were Bendtsen air permeability (B_air_p), average pore diameter (Av_PoreD), Bendtsen roughness (B_rough), $\theta_a$ roughness ($\theta_a$), contact angle (Cont_ang), and pH of the coating color (pH_color). Separate PLS models (Table IV) were calculated for both PVA-poly-DADMAC and weakly cationic SA latex-starch coating sets, because the model including all the coatings was found to explain mainly the differences between the wettability of the two polymer systems.

#### *PVA-poly-DADMAC Coatings*

The PLS model for PVA-poly-DADMAC coatings consists of three principal components (PC) and explains altogether 66.3% of the variation of Y variables ($R^2$YCum). The eigenvalue of PC3 is smaller than 1, so this component can be neglected in the further discussions of the results. The PLS weight plot presented in Fig. 3 illustrates the relationships between the physical properties

**TABLE IV. PLS Models for PVA-poly-DADMAC and Weakly Cationic SA Latex–Starch Coatings. $R^2X$, $R^2Y$ and $Q^2$ Denote the Explained Variation of X- and Y-Variables, and the Predicted Variation, Respectively.**

| Polymer system | PC | $R^2X$ | $R^2XCum$ | Eigenvalue | $R^2Y$ | $R^2YCum$ | $Q^2$ | $Q^2Cum$ |
|---|---|---|---|---|---|---|---|---|
| PVA-poly-DADMAC | 1 | 0.596 | 0.596 | 3.579 | 0.168 | 0.168 | –0.278 | 0.000 |
| | 2 | 0.241 | 0838 | 1.449 | 0.215 | 0.383 | –0.069 | 0.000 |
| | 3 | 0.100 | 0.938 | 0.599 | 0.281 | 0.663 | –0.036 | 0.000 |
| SA latex–starch | 1 | 0.649 | 0.649 | 3.896 | 0.680 | 0.680 | 0.505 | 0.505 |
| | 2 | 0.217 | 0.867 | 1.303 | 0.080 | 0.761 | –0.128 | 0.505 |
| | 3 | 0.114 | 0.980 | 0.683 | 0.093 | 0.854 | –0.006 | 0.505 |

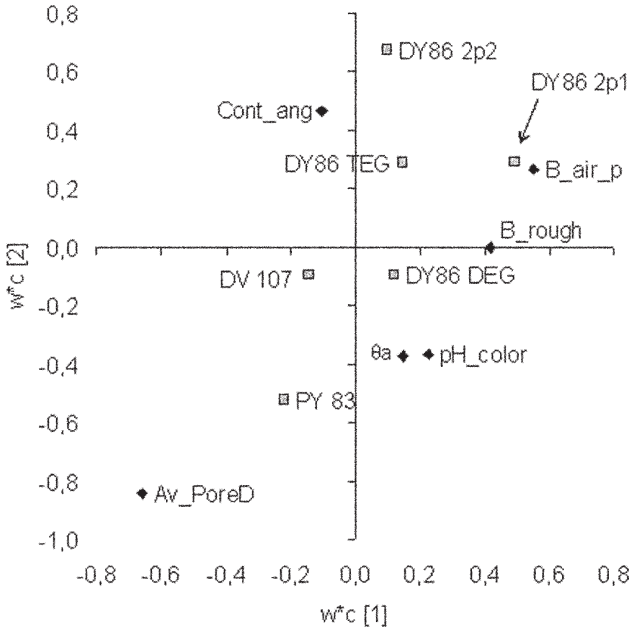


**Figure 3.** PLS weights for the effect of coating properties on water fastness on PVA-poly-DADMAC coatings.

of the model coatings (X variables) and water fastness values (Y variables) in terms of the first and second principal components. The plot can be interpreted as follows: Firstly, a straight line is imagined going from one Y variable through the plot origin and secondly, all the X variables are projected orthogonally onto this imaginary line. The distance of each projection from the origin determines the contribution (weight) of the corresponding X variable to the Y variable, such that the longer the distance, the stronger the contribution.

Figure 3 indicates that the first principal component PC1 separates the DY 86 inks from DV 107 and PY 83 inks to the positive side of the origin. In the direction of the second principal component PC2, the pigmented ink PY83 is located below the dye-based inks. However, the latter do not form a distinct group, which suggests that the contributions of various X variables differ depending on the ink's composition. Regardless of this, some general trends can be suggested. For all the studied inks, the most significant factor influencing water fastness on PVA-poly-DADMAC coatings appears to be the average pore diameter (Av_PoreD) of the coating. Also Bendtsen air permeability (B_air_p) and Bendtsen roughness (B_rough) have some relevance, whereas the contribution of the surface chemical properties (Cont_ang, pH_color) is not unambiguous.

With soluble DY 86 inks, water fastness is improved as the Bendtsen air permeability and Bendtsen roughness decrease and average pore diameter increases. This would suggest that water fastness improves as the coating structure becomes more dense. However, for DV 107 ink based on modified soluble dye and pigmented ink PY 83, the opposite is true. One possible explanation for this could be the different nature of the studied colorants. The dye-based colorants generally tend to penetrate into the coating layer with the carrier phase, whereas pigment particles are commonly thought to form a filter cake on top of the pigment coating. Some evidence on this kind of behavior can be found from the Raman depth profiles presented in Fig. 4. The profiles were measured from dye-based and pigment-based prints on PVA-poly-DADMAC coating containing 100 pph PCC. Figure 4 shows that the dye-based DY 86 colorant has penetrated deeper into the coating than the pigmented ink PY 83, as the widths of the colorant profiles differ. In the case of DY 86, the main profile is approximately 10 μm wide, whereas in the case of PY 83, the profile it is only about 5 μm.

Summarizing, the data would suggest that the model inks based on the DY 86 colorant would benefit from an impermeable coating structure which would be able to protect the colorant from exposure to water. In contrast, a coarser coating would be advantageous for pigmented inks, because this would make it easier for the pigment particles to penetrate deeper into the coating structure. It should be born in mind, though, that these experimental inks did not contain additional surfactants, which undoubtedly affects the physical paper–ink interactions. Furthermore, the water fastness of all the studied model inks was very good, irrespective of the PCC:kaolin pigment ratio, which would indicate that on PVA-poly-DADMAC coatings chemical paper–ink interactions are more important than the studied physical properties of the coating. This is supported by the fact that the explained variation of Y variables ($R^2YCum$) after two principal components is only 38.3%, and the model does not predict the data variation ($Q^2Cum$) at all.

### *Weakly Cationic SA Latex-Starch Coatings*

The PLS model for the weakly cationic SA latex-starch coatings presented in Table IV consists of three principal components that explain altogether 85.4% of the variation of Y variables and predict 50.5% of the data variation. This is clearly better than in the case of PVA-poly-DADMAC coatings. Again, the eigenvalue of PC3 is smaller than 1, so it can be excluded from the further discussion. The resulting PLS weight plot for the first two principal components is presented in Fig. 5. PC1 explains 68.0% of the variation in water fastness values, but does not separate various inks from each other. This indicates that, in terms of the first principal component, all the studied coating-related variables have a similar influence on water fastness, irrespective of the

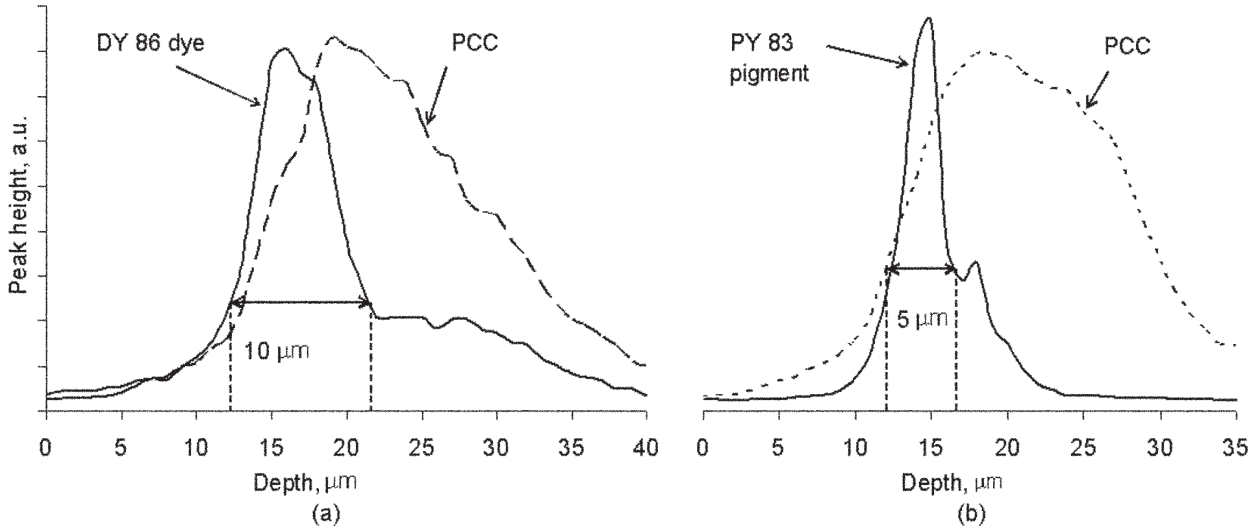


**Figure 4.** Raman depth profiles of untreated prints: a) DY86 2p2 and b) PY83. Model coating P100:0.

type of model ink. The $R^2Y$ component of PC2 is much smaller that that of PC1, as it explains only 8.0% of the variation in water fastness values. The inks containing 2-pyrrolidone as a co-solvent (DY 86 2p1, DY 86 2p2, DV 107) are positioned on the negative side of the PC2 axis, whereas the others are on the positive side.

The PLS weight plot presented in Fig. 5 indicates that the four most important properties of the weakly cationic SA latex-starch coatings affecting water fastness are Bendtsen roughness (B_rough), average pore diameter (Av_PoreD), Bendtsen air permeability (B_air_p) and pH of the coating color (pH_color). In contrast, the contributions of $\theta_a$ roughness ($\theta_a$) and contact angle (Cont_ang) seem to be rather small. To be more specific, the data implies that the water fastness of the studied model inks is generally improved as the roughness, porosity, and pH value of the coating color decrease, and as average pore diameter increases. These structural changes can be related to an increase in the proportion of kaolin in the coating. They also support the idea that a more impermeable coating would protect the printed image against water. Thus, in the case of the weakly cationic SA latex-starch coatings, the structural properties of the coating appear to be more significant for the water fastness of the studied model inks than the hydrophobicity of the coating.

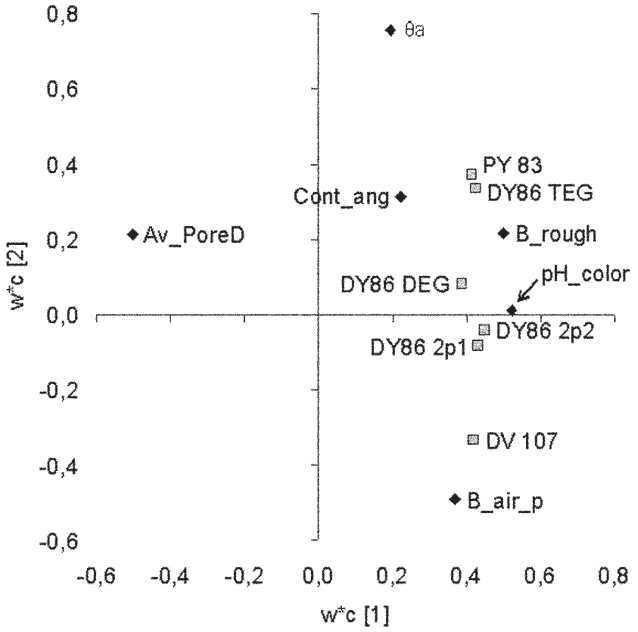


**Figure 5.** PLS weights for the effect of coating properties on water fastness on weakly cationic SA latex-starch coatings.

## Chemical Paper–Ink Interactions on PVA-poly-DADMAC Coatings

The results of the PLS analyses (Table IV and Fig. 3) suggest that the structural properties of the PVA-poly-DADMAC coatings have only a minor influence on the water fastness of the studied ink jet prints. Consequently, the effect of chemical paper–ink interactions on water fastness was explored by recording FTIR-ATR spectra of untreated and water-immersed prints using a diamond microcrystal. Spectral analysis was carried out with principal component analysis (PCA). An example of the results representing the common behavior of all the studied PVA-poly-DADMAC coatings is presented in Fig. 6. The horizontal axis of the plot stands for the spectral wavenumbers and the vertical axis for the loading values, or the magnitudes of contribution of each wavenumber. In this illustration, the positive loadings represent the contributions typical for untreated prints and negative loadings for water-immersed prints. The contributions at the wavenumber regions 2400–2300 $cm^{-1}$ and 2300–1800 $cm^{-1}$ originate from the atmospheric $CO_2$ and the dead spot of the diamond ATR-crystal, respectively, and can be neglected in the further discussion.

Figure 6 demonstrates that untreated and water-immersed prints differ in terms of the contributions related to PVA and the DY 86 colorant. Contributions on the positive side of the loading plot represent untreated prints and they may conceivably be associated with various vibrational modes of PVA polymer as follows[23]: O–H stretching of hydrogen bonded OH groups at 3600–3100 $cm^{-1}$; C–H stretching of alkyl groups at 3000–2800 $cm^{-1}$; CH+OH bending at 1443 $cm^{-1}$ and 1327 $cm^{-1}$; $CH_2$ bending at 1427 $cm^{-1}$; $CH_2$ wagging at 1367 $cm^{-1}$; C–O–

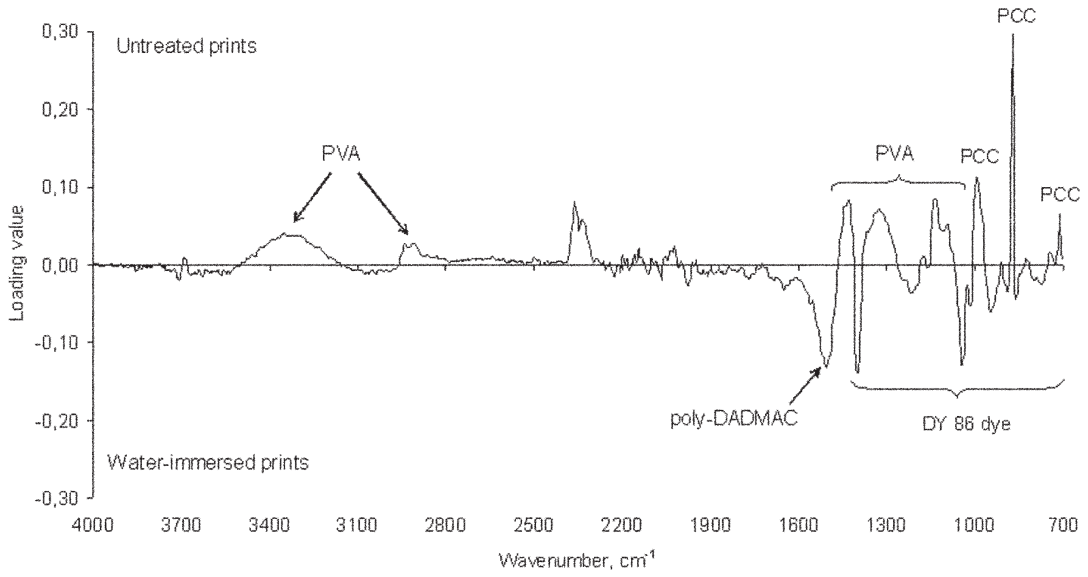


**Figure 6.** Loading values of untreated and water-immersed prints (all DY 86 inks, all PVA-poly-DADMAC coatings).

C stretching at 1134 $cm^{-1}$; C–O stretching at 1091 $cm^{-1}$; skeletal vibrations at 910 $cm^{-1}$ and 848 $cm^{-1}$; $CH_2$ rocking at 825 $cm^{-1}$. Besides PVA, contributions originating from PCC pigment can also be observed on the positive side of the loading plot. Possible assignments for these could be out-of-plane and in-plane deformations of $CO_3^{2-}$ at 872 $cm^{-1}$ and 710 $cm^{-1}$, respectively.[24]

The negative side of the loading plot represents water-immersed prints, and is governed by several bands originating from the DY 86 dye. These appear mainly in the wavenumber region 1400–700 $cm^{-1}$. Possible assignments[24,25] for these could be C–H bending of methylene groups at 1400 $cm^{-1}$, symmetric and asymmetric S–O stretching, and S–C stretching of the sulfonate group at 1246 $cm^{-1}$, 1196 $cm^{-1}$, and 1042 $cm^{-1}$, respectively, and out-of-plane vibrations of aromatic rings at 890 $cm^{-1}$ and 801 $cm^{-1}$. The other negative loadings can presumably be assigned to poly-DADMAC. In particular, the contributions at 1504 $cm^{-1}$, 1015 $cm^{-1}$ and 945 $cm^{-1}$ could perhaps be associated with various vibrational modes of $C–N(CH_3)_3$ group.[24] Consequently, the spectral changes illustrated in Fig. 6 would suggest at least partial dissolution of PVA from the coating during the exposure to water, whereas the dye would still be retained in the coating. Some evidence on this kind of behavior could also be seen in the previous study.[14] Moreover, the dissolution of the PVA binder could partly explain the poor correlation between the structural properties of the PVA-poly-DADMAC coating and the water fastness values.

Despite the apparent dissolution of PVA binder as a result of water immersion, the water fastness of all the studied prints is very good, as Fig. 1 and Table III indicate. Previous studies[6,14,17] have suggested that anionic dye-based colorants tend to form ionic bonds with cationic coatings, which would strongly counteract dye dissolution and enhance water fastness. Indications on this kind of behavior can also be found from the FTIR spectral data of the present study. Figure 7 presents the FTIR-DTGS spectrum of dried DY 86 colorant (the upper curve) and the PCA loading values of printed DY86 DEG ink (the lower curve). The latter is obtained by comparing the FTIR-ATR spectra of unprinted coatings with the corresponding printed ones. The DY 86 colorant

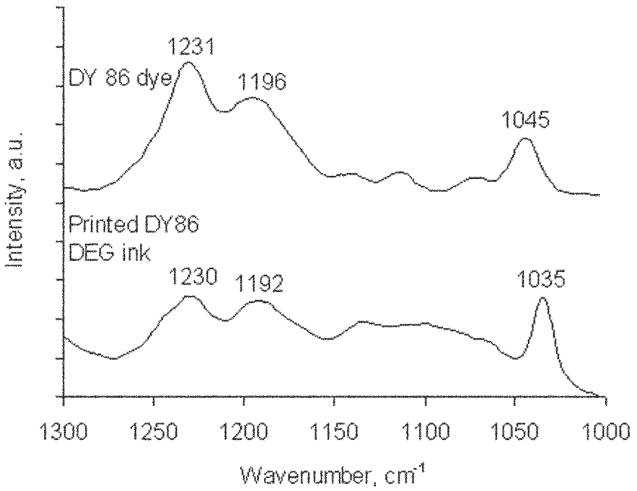


**Figure 7.** FTIR-DTGS spectrum of the dried direct dye DY 86 (upper) and the PCA loading values of printed DY86 DEG ink (lower).

contains sulphonic acid groups attached directly to the aromatic backbone of the colorant molecule ($Ar-SO_3^-$). According to the literature,[24] the FTIR bands originating from the aromatic sulphonic acid salts appear approximately at the wavenumbers 1230, 1190, 1130 and 1040 $cm^{-1}$. These bands have been associated to three SO and S-phenyl vibrations interacting. Consequently, in the DTGS spectrum of the dried dye, the bands at 1231 and 1196 $cm^{-1}$ could originate from symmetric and asymmetric S–O stretching and the band at 1045 $cm^{-1}$ from S–C stretching between the sulfur atom and aromatic ring.

Comparison of the two spectra, as presented in Fig. 7, reveals that in the PCA loading curve representing the printed dye, the bands related to aromatic sulfonic acid salts have shifted to lower wavenumbers. This is the common behavior of all the studied DY86 inks, though the magnitude of the shift depends on the ink-coating combination in question. One conceivable explanation for the band shifts might be weakening of the

S–C bond between the sulfur atom and aromatic ring owing to ionic interaction between the oxygen of the anionic sulfonic acid group and cationic groups of the coating. In this case, the sulfonic acid group would act as an electron donor, when its electrons would move towards the electron acceptors of the coating (cationic groups). Consequently, the strengths of S–C and S–O bonds in the sulphonic acid group would decrease. This would suggest that the studied anionic DY86 dye molecules would primarily be attached to cationic coating with ionic bonds, which would strongly resist dye dissolution and enhance water fastness.

### Chemical Paper–Ink Interactions on Weakly Cationic SA Latex-Starch Coatings

The water fastness data presented in Table III suggested that the water fastness of the studied model ink jet inks improves as the amount of kaolin increases in the coating. Visual inspection of the water-immersed samples revealed that bleeding of DY 86 and DV 107 dyes is clearly more pronounced on weakly cationic latex-starch coatings than on PVA-poly-DADMAC coatings, regardless of the pigment ratio of the coating, or ink solvent composition. This suggests that the dyes are at least partially attached to a component that dissolves during water treatment. A previous study[26] suggested that the studied dye-based model inks were mainly attached to the coating polymers instead of the pigment. Evidence of this kind of behavior can also be found from the present data, as is illustrated in Fig. 8 presenting a Raman depth profile measured from an untreated model coating S80:20 printed with the DY 86 DEG ink. It is obvious that the distribution of the DY 86 dye overlaps mostly with the distributions of coating polymers. This would infer that in an untreated print the dye is mainly attached to the coating polymers. This is a common behavior of all the studied coatings independent of the pigment ratio. Note should nevertheless be taken of the fact that detection of kaolin and starch from the Raman spectra of the prints was substantially complicated by intensive fluorescence. Moreover, their Raman bands overlapped notably with the dye and other coating components. These factors undoubtedly weaken the reliability of the observations.

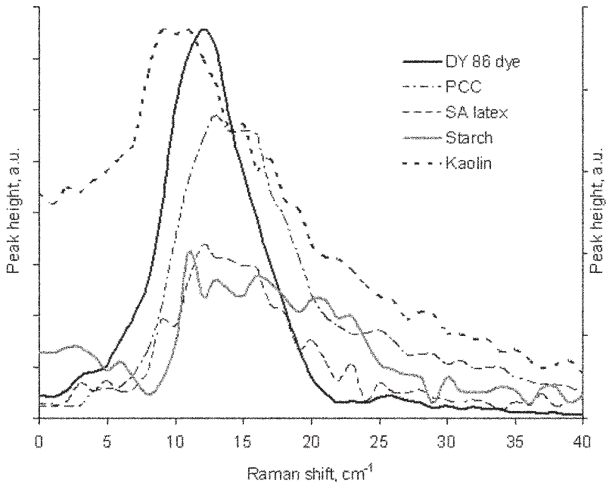


**Figure 8.** Raman depth profile of an untreated print. Model coating: S80:20, model ink: DY 86 DEG.

To analyze the effects of water treatment on the printed samples, PCA analysis was performed for the FTIR-ATR spectra of untreated and water-immersed prints. Figure 9 shows an example of the results. The PCA plot is obtained by comparing the FTIR-ATR spectra measured from untreated and water-immersed prints when DY 86 DEG ink is used. The positive loading values of the plot represent the untreated prints, whereas the negative values stand for the water-immersed prints. Contributions on the positive side of the loading plot can conceivably be associated with various vibrational modes of the DY 86 dye, starch and the coating pigments. The contributions at 1393 $cm^{-1}$, 1230 $cm^{-1}$, 1190 $cm^{-1}$ and 1038 $cm^{-1}$ represent likely the DY 86 dye, in which case the latter three could possibly be related to the aromatic sulphonic acid salts.[24] Other contributions on the positive side of the loading plot are located at 1177 $cm^{-1}$, 1138 $cm^{-1}$, 1115 $cm^{-1}$, 1096 $cm^{-1}$, 1080 $cm^{-1}$ and 999 $cm^{-1}$. Both starch and kaolin have strong, markedly overlapping absorptions in this

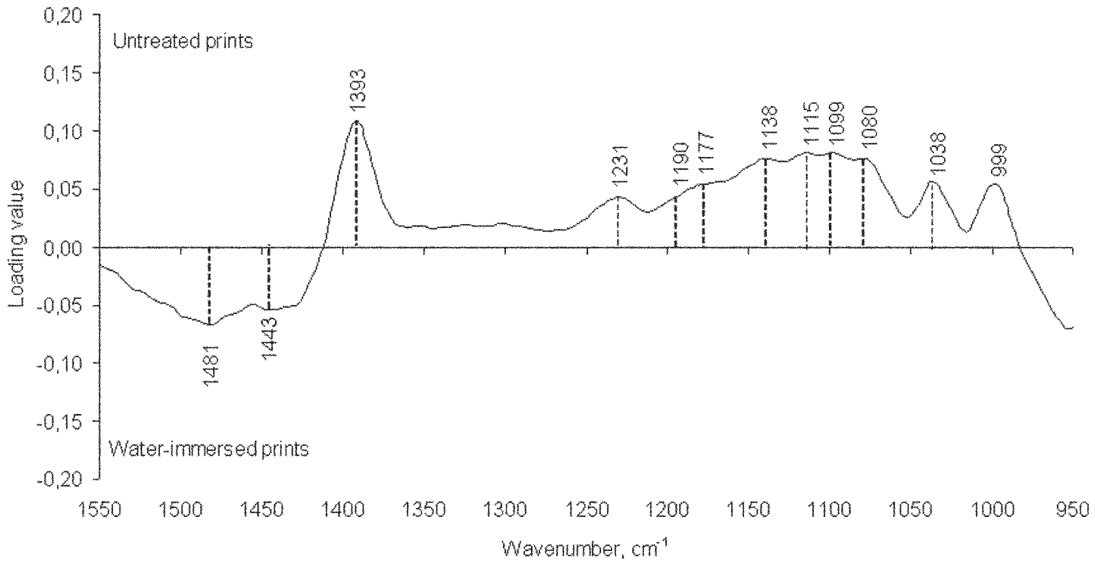


**Figure 9.** PCA loading values of untreated and water-immersed prints, when DY86 DEG ink is used.

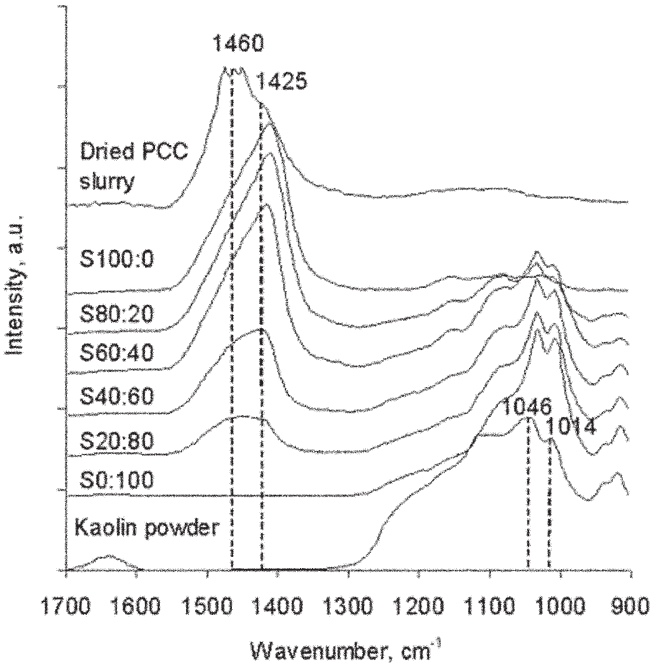


**Figure 10.** FTIR spectra of kaolin powder, untreated coatings S0:100…S100:0, and dried PCC slurry. The spectra are vertically shifted for clarity.

wavenumber region, representing C–O and Si–O vibrations, respectively. In particular, the band at 1080 $cm^{-1}$ might originate from an asymmetric stretching of the glucose ring in starch, whereas the band at 999 $cm^{-1}$ could represent kaolin.[24,27,28] Furthermore, the DY 86 dye and PCC have weak IR bands in this region. On the negative side of the plot, the loadings at 1481 $cm^{-1}$ and 1443 $cm^{-1}$ might represent SA latex.[24,29] This would suggest that starch and dye are more abundant in the untreated prints than in the water-immersed prints, whereas the latex would be retained in the coating even after water treatment.

Moreover, the contributions associated with the DY 86 colorant (Fig. 9) infer that the dye interacts with the coatings. Comparison of these values to the FTIR-DTGS spectrum of the dried DY 86 dye in Fig. 7 reveals that the bands have shifted to lower wavenumbers. Especially, the peaks representing symmetric and asymmetric S–O stretching have shifted from 1231 $cm^{-1}$ to 1230 $cm^{-1}$ and 1196 $cm^{-1}$ to 1190 $cm^{-1}$, and the S–C stretching band from 1045 $cm^{-1}$ to 1038 $cm^{-1}$. Figure 8 already demonstrated that the dye appears to be primarily associated with the coating polymers, so these shifts could perhaps originate from ionic interaction of the sulphonic acid groups of the dye with the quaternary ammonium groups ($NR_4^+$) of starch or latex. It should be noted, however, that various strong bands originating from dye, kaolin, latex and starch overlap substantially with each other in the wavenumber range 1300–1000 $cm^{-1}$. This complicates detailed detection of the band positions.

Besides the structural factors, the chemical properties of the coating layer may vary with the pigment ratio of the coating. This could influence the adhesion between the dye and the coating, and thus also have an effect on water fastness. As the studied dyes appear to be mainly attached to the coating polymers, it is suggested that on latex-starch coatings, water fastness would be related to the affinity of the coating polymers to the pigments. In the case of weakly cationic SA latex-starch coatings, the coating color ingredients were added in the following sequence: 1) pigments, 2) weakly cationic starch, 3) weakly cationic SA latex and 4) CMC thickener as a powder. The starch should thus be able to interact with the coating pigments before the other chemicals. Moreover, the SA latex used in this study is stabilized with cationic starch. Kaolin is more anionic than PCC, as their measured zeta potentials are –31.1 mV and –4.9 mV, respectively. According to the literature,[30] kaolin particles are generally anionic in the pH range of this study, whereas the isoelectric point of calcite is 8.2., and in alkaline solutions this mineral becomes more negative and the solution more acidic over time.[31] Consequently, the PCC particles can be assumed to be weakly cationic in the pH range of the model coatings used in this study (Table I).

With regard to the interactions between starch and coating pigments, both cationic and amphoteric starches have been found to adsorb strongly on kaolin particles.[32] In contrast, another study[33] has demonstrated that the interaction between cationic starch and calcium carbonate weakens as the density of cationic surface sites increases when $CaCl_2$ is added to the system. Therefore, one possible explanation for the better water fastness of the studied dye-based model inks on the coatings S0:100 and S20:80 could be the stronger interaction between starch and kaolin particles than between starch and PCC particles. Furthermore, as the proportion of kaolin increases in the coating, the pH increases and PCC particles become more anionic. This could enhance the interaction also between PCC and starch and thereby reduce the dissolution of starch and dye from the coating.

Some indications of variable interactions between the coating polymers and pigments can be observed from the FTIR spectra measured from the coating pigments and unprinted coatings (see Fig. 10). Namely, the positions of the major bands of PCC and kaolin seem to be dependent on the PCC:kaolin ratio of the coating. In the FTIR spectrum of dried PCC slurry, there are two strong, overlapping bands,[24] representing the asymmetric out-of-phase stretch of $CO_3^{2-}$, approximately at wavenumbers 1460 and 1425 $cm^{-1}$. In the coating S100:0, the corresponding bands lie at 1443 and 1412 $cm^{-1}$. The decreases in the wavenumbers indicate an interaction of PCC with the other coating components, that is to say, polymers. As the proportion of the kaolin increases in the coating, the PCC bands shift gradually towards higher wavenumbers. For example, in the coating containing 20 pph PCC and 80 pph kaolin (S20:80), the PCC bands are located approximately at 1450 and 1426 $cm^{-1}$. This alludes that the interaction of PCC with the coating polymers has diminished as a result of kaolin addition.

Corresponding shifts of certain kaolin bands can be observed as well. In the FTIR spectrum measured from the kaolin powder, the bands related to Si–O stretching vibrations[24,28] are at wavenumbers 1046 and 1014 $cm^{-1}$. In the coating containing 100 pph kaolin (S0:100), the corresponding bands lie at lower wavenumbers, viz. 1030 and 1007 $cm^{-1}$. Again, this would suggest interactions with the coating polymers. As the proportion of kaolin decreases in the coating, a gradual shift of these bands to higher wavenumbers can be observed. In the coating containing 80 pph PCC and 20 pph kaolin (S80:20), the bands are positioned at 1034 $cm^{-1}$ and 1011 $cm^{-1}$. These are closer to the values of the kaolin powder than those of the S0:100 coating.

These observations suggest that kaolin and PCC compete for the coating polymers at least to some extent. The large shifts of the kaolin bands would infer that the weakly cationic polymers used in this study tend to interact more strongly with the colors containing large amounts of kaolin, perhaps because of the more anionic nature of the pigments at higher pH levels. To summarize, the results indicate that the DY86 dye is at least partly attached to the starch, whereas the interactions between starch and the other coating components, or between dye and starch, are not strong enough to counteract dissolution. Consequently, the water fastness of the ink jet prints is impaired.

## Conclusions

The purpose of this study was to examine the water fastness of ink jet prints on model coatings consisting of PCC and kaolin pigments intended particularly for ink jet printing. The contributions of the physical properties of the coating and of chemical paper–ink interactions were of particular interest. These were studied using conventional methods for measuring paper properties and print quality, FTIR and Raman spectroscopy, and multivariate data analysis methods.

The PCC:kaolin ratio of the coating did not have a marked effect on the water fastness of the studied model inks on PVA-poly-DADMAC coatings. However, on weakly cationic SA latex-starch coatings a high proportion of kaolin proved to be beneficial. The water fastness of the dye-based model inks was found to be considerably better on PVA-poly-DADMAC coatings than on weakly cationic SA latex-starch coatings, despite the clearly more hydrophobic nature of the latter. Thus, the wettability of the coating was suggested to be a minor factor affecting the water fastness of the dye-based model inks within the studied sample set. The coating composition did not have any major effect on the water fastness of the pigmented ink examined in the present study.

The PLS analysis indicated that in the case of PVA-poly-DADMAC coatings, the contribution of the physical properties of the coating to the water fastness was generally small, but nevertheless appeared to be somewhat dependent on the type of colorant. The PVA binder proved to dissolve at least partially from the coating as a result of exposure to water, which could in part explain the poor correlation between the physical properties of the coating and water fastness. The role of chemical paper–ink interactions, namely ionic bonding, proved to be decisive for the development of the water fastness of the studied model inks.

In the case of weakly cationic latex-starch coatings, the physical properties of the coating layer were found to contribute much more to the water fastness of the studied model inks. Water fastness was improved as the roughness, porosity, and pH value of the coating color decreased and the average pore diameter increased, supporting the assumption that an impermeable coating would protect the printed image against water. With regard to the chemical paper–ink interactions on weakly cationic latex-starch coatings, the water fastness of the studied dye-based model inks was suggested to be related to the affinity of the coating polymers, particularly starch, to the coating pigments.

To summarize, the results obtained with the experimental coatings and inks suggested that the chemical paper–ink interactions played a dominant role for the effect on water fastness, whereas the role of physical paper properties depended on the type of coating. Ionic interactions between the dye and the coating appeared to be generally beneficial, but not necessarily adequate to guarantee good water fastness, particularly if the interactions occur between the dye and some water-soluble component of the coating.

**Acknowledgment.** The authors would like to thank Ms. Liisa Hakola, Ms. Tuire Toivonen and Ms. Mervi Sillman in HUT's Laboratory of Media Technology, and Ms. Marja Kärkkäinen and Mr. Timo Pääkkönen in HUT's Laboratory of Forest Products Chemistry for their skillful assistance in the laboratory work. Raisio Chemicals is acknowledged for providing the coating polymer needed for the study. Financial support from the National Technology Agency of Finland (TEKES), M-Real, UPM-Kymmene, Stora Enso, Raisio Chemicals, and the International Ph.D. Programme in the Pulp and Paper Science and Technology (PaPSaT) is gratefully acknowledged.

## References

1. D. Glittenberg, A. Voigt, and D. Donigian, *Wochenblatt Papierfabr.* **130**, 1279 (2002).
2. D. E. Bugner, in *Handbook of imaging materials*, Marcel Dekker, New York, 2002, pp. 603–628.
3. D. M. Chapman and D. Michos, *J. Imaging Sci. Technol.* **44**, 418 (2000).
4. D. Glittenberg and A. Voigt, *Paper Tech.* **42**, 24 (2001).
5. D.I. Lunde, *Pulp Paper*, 41 (May, 1999).
6. R. Y. Ryu, R. D. Gilbert, and S. A. Khan, *Tappi J.*, **82**, 128 (1999).
7. B. E. Yoldas, *J. Sol-Gel. Sci. Tech.*, **13**, 147 (1998).
8. R. Sangl, O. Wittig, and J. Weigl, in *Proc. IS&T's NIP13 Congress*, IS&T, Springfield, VA 1997, pp. 460–465.
9. M. C. Withiam, in *Proc. IS&T's NIP12 Congress*, IS&T, Springfield, VA 1996, pp. 409–417.
10. A. Lavery and S. Spittles, in *Proc. IS&T's NIP17 Conference,* IS&T, Springfield, VA 2001, pp. 226–230.
11. R. N. Jopson, in *Proc. 2001 Coating and graphic arts conference and trade fair*, TAPPI Press, Atlanta, GA 2001, pp. 163–182.
12. M. Londo, *Pulp Paper*, 37 (May, 2000).
13. J. E. Cawthorne Jr., M. Joyce, and D. Fleming, *J. Coat. Tech.* **75**, 75 (2003).
14. K. Vikman, *J. Imag. Sci. Technol.* **47**, 38 (2003).
15. K. Vikman, in *Proc. IS&T's NIP18 Conference,* IS&T, Springfield, VA 2002, pp. 408–413.
16. K. Khoultchaev and T. Graczyk, *J. Imaging Sci. Technol.* **45**, 16 (2001).
17. L. Shaw-Klein, *Proc. IS&T's NIP14 Conference*, IS&T, Springfield, VA 1998, pp. 129–132.
18. H. A. Willis, J. H. van der Maas and R. G. J. Miller, Eds., *Laboratory Methods in Vibrational Spectroscopy*, John Wiley and Sons, London, 1987, p. 545.
19. J. Vyörykkä, M. Halttunen, H. Iitti, E. Kenttä, J. Paaso, J. Tenhunen, T. Vuorinen, and P. Stenius, in *Proc. 2001 Coating and graphic arts conference and trade fair*, TAPPI Press, Atlanta, GA 2001, pp 193–201.
20. L. Eriksson, E. Johansson, N. Kettaneh-Wold, and S. Wold, *Multi- and Megavariate Data Analysis. Principles and Applications*, Umetrics Academy, Sweden, 2001, p. 533.
21. A. Hladnik and T. Muck, *Dyes Pigm.*, **54**, 253 (2002).
22. P. L. Lang, J. Cook, B. Fuller, M. Scott, C. S. Telles, and T. Barrett, *Appl. Spectr.* **52**, 713 (1998).
23. T. F. Cooney, L. Wang, S. K. Sharma, R. W. Gauldie, and A. J. Montana, *J. Polym. Sci. B*, **32**, 1163 (1994).
24. N. B. Colthup, L. H. Daly and S. E. Wiberley, Eds., *Introduction to Infrared and Raman Spectroscopy*, Academic Press, Inc., San Diego, USA, 1990, p. 310.
25. D. Lin-Vien, N. B. Colthup, W. G. Fateley, and J. G. Grasselli, Eds., *The Handbook of Infrared and Raman Characteristic Frequencies of Organic Molecules,* Academic Press, San Diego, CA, 1991.
26. K. Vikman, *J. Imag. Sci. Technol.* **47**, 30 (2003).
27. K. K. Pandey, *J. Appl. Polym. Sci.*, **71**, 1969 (1999).
28. V. C. Farmer and J. D. Russell, *Spectrochim. Acta*, **20**, 1149 (1964).
29. I. Mathakiya, P. V. C. Rao, and A. K. Rakshit, *J. Appl. Polym. Sci.*, **79**, 1513 (2001).
30. G. Drage and O. Tamms, in *Pigment Coating and Surface Sizing of Paper. Papermaking science and technology,* Fapet, Helsinki, Finland, 2000, pp. 68–92.
31. P. Somasundaran and G. E. Agar, *J. Coll. Int. Sci.*, **24**, 433 (1967).
32. X.-Q. Wang, J. Grön and D. Eklund, *J. Pulp Pap. Sci.*, **22**, J486 (1996).
33. F. Hedborg and T. Lindström, *Nord. Pulp Pap. Res. J.*, **8**, 319 (1993).